Electronic correlation and strain effects at the interfaces between polar and nonpolar complex oxides

A. Annadi,[1,2] A. Putra,[1,3] Z. Q. Liu,[1,2] X. Wang,[1,2] K. Gopinadhan,[1,4] Z. Huang,[1] S. Dhar,[1,4] T. Venkatesan,[1,2,4] and Ariando[1,2,*]

[1]*NUSNNI-Nanocore, National University of Singapore, 117411 Singapore*

[2]*Department of Physics, National University of Singapore, 117542 Singapore*

[3]*Department of Engineering Science Programme, National University of Singapore, 117576 Singapore*

[4]*Department of Electrical and Computer Engineering, National University of Singapore, 117576 Singapore*

(Received 27 April 2012; published 27 August 2012)

The interface between the polar $LaAlO_3$ and nonpolar $SrTiO_3$ layers has been shown to exhibit various electronic and magnetic phases such as two-dimensional electron gas (2DEG), superconductivity, magnetism, and electronic phase separation. These rich phases are expected due to the strong interplay between charge, spin, and orbital degree of freedom at the interface between these complex oxides, leading to the electronic reconstruction in this system. However, until now all of these new properties have been studied extensively based on the interfaces which involve a polar $LaAlO_3$ layer. To investigate the role of the ABO_3 polar layer, here we study various combinations of polar/nonpolar oxide ($NdAlO_3/SrTiO_3$, $PrAlO_3/SrTiO_3$, and $NdGaO_3/SrTiO_3$) interfaces which are similar in nature to the $LaAlO_3/SrTiO_3$ interface. Our results show that all of these new interfaces can also produce 2DEG at their interfaces, supporting the idea that the electronic reconstruction could be the driving mechanism for the creation of the 2DEG at these oxide interfaces. Furthermore, the electrical properties of these interfaces are shown to be governed by the interface strain and the type of cations in the polar overlayers. Our observations may provide an approach to further tune the properties of the 2DEG at the selected polar/nonpolar oxide interfaces.

DOI: 10.1103/PhysRevB.86.085450 PACS number(s): 73.40.Rw, 68.47.Gh, 73.20.Hb, 73.50.Gr

I. INTRODUCTION

Heterostructures constructed from polar/nonpolar oxides, especially the $LaAlO_3/SrTiO_3$ interface, have been a topic of research in recent years in which along with two-dimensional electron gas (2DEG), novel properties have been reported.[1–5] Further, it has been demonstrated that the properties at the $LaAlO_3/SrTiO_3$ interface can be manipulated in many ways such as the electric field effect,[2] atomic force microscopy (AFM) charge writing,[6] and adsorbate capping,[7] showing the ability to tune the interface by external parameters. Moreover, in the $LaAlO_3/SrTiO_3$ heterostructure the combined effects of lattice mismatch (∼2.3%) between $LaAlO_3$ and $SrTiO_3$ and the electronic effects provided by polar $LaAlO_3$ at the interface play a strong role in controlling the interface properties. Recently, Bark *et al.*[8] demonstrated strain effects on properties of 2DEG at the $LaAlO_3/SrTiO_3$ interface by growing the heterostructure on different substrates. In addition to this, electrostriction and electromechanical response were demonstrated at the $LaAlO_3/SrTiO_3$ heterostrures.[9,10] Recently, a similar 2DEG was also shown to exist at the $LaGaO_3/SrTiO_3$ interface.[11] In all the above observations, the polar nature of the overlayer is critical. The significance of the polar overlayer can be further explored by investigating various new combinations of polar/nonpolar oxide heterostructures. In this scenario, a choice of variety in chemical nature and lattice structure of polar layers enables us to tune the interface properties. Moreover this approach may help in revealing key issues such as the driving mechanism of the formation of 2DEG which is widely believed to originate from polarization catastrophe[12] due to the polar/nonpolar nature of the interface and the localization of carriers at this interface due to the lifting of the degeneracy of the Ti *d* states. In this article, we investigate various combinations of polar/nonpolar oxide interfaces [Fig. 1(a)] $REBO_3/SrTiO_3$ (100) (RE = La, Pr, or Nd, B = Al or Ga) and study their structural and electrical properties. The choice of polar oxides is made in such a way that all of them are similar to $LaAlO_3$ in nature, having $(AO)^{+1}$ and $(BO_2)^{-1}$ polar charge layers alternatively along the (100) direction.

II. EXPERIMENTAL

Samples were prepared by pulsed laser deposition, ablating $REBO_3$ targets onto TiO_2-terminated $SrTiO_3$ (100) substrates. Atomically flat TiO_2-terminated $SrTiO_3$ (100) substrates were obtained by employing well-established conditions: buffered hydrofluoric (HF) acid treatment for 30 s followed by thermal annealing at 950 °C for 2 h.[13,14] Samples were prepared in a range of oxygen partial pressure (P_{O_2}) of 1×10^{-3} to 1×10^{-5} Torr at 800 °C. The laser (248 nm) energy density was 1.4 J/cm^2 and the repetition rate was 1 Hz. During deposition, the film growth and the number of unit cells were monitored by *in situ* reflection high-energy electron diffraction (RHEED). Samples with thicknesses ranging from 1 to 14 unit cells (uc) were grown for $NdAlO_3$ while a fixed 10 uc was used for all other polar layers for comparison. Epitaxial growth of films on $SrTiO_3$ substrates were further confirmed by high-resolution x-ray diffraction (HRXRD). Electrical contacts were made with an Al wire bonding directly to the interface. Sheet resistance and Hall effect measurements were carried out to extract carrier density, mobility, and electrical properties. Figure 1(b) shows RHEED intensity patterns obtained during the growth of the samples, clearly showing the layer by layer growth mode for various polar oxide layers on $SrTiO_3$. Figure 1(c) shows an AFM topography image after the growth of 10 uc $NdAlO_3$ on $SrTiO_3$ with preserved steps and further

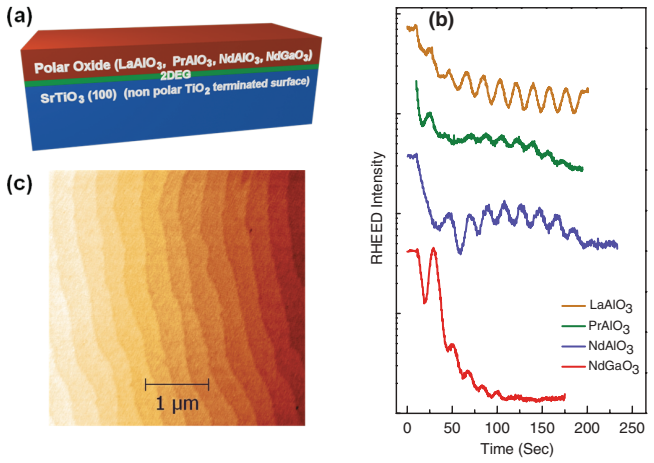

FIG. 1. (Color online) (a) Schematic representation of polar/nonpolar REBO_3/$SrTiO_3$ (RE, Rare earth element) heterostructure. (b) Typical RHEED oscillations obtained for the growth of different polar layers on top of TiO_2-terminated $SrTiO_3$ substrate. (c) AFM image of a 10-uc $NdAlO_3$/$SrTiO_3$ sample showing an atomically smooth surface.

confirms the layer by layer growth. Even though all these polar oxides offer substantial lattice mismatch with the $SrTiO_3$ substrate, we have successfully grown them by optimizing deposition conditions.

III. RESULTS AND DISCUSSION

We first discuss the case of the $NdAlO_3$/$SrTiO_3$ interface. Figure 2(a) shows the dependence of sheet resistance, R_s, on temperature for the $NdAlO_3$/$SrTiO_3$ interface prepared in

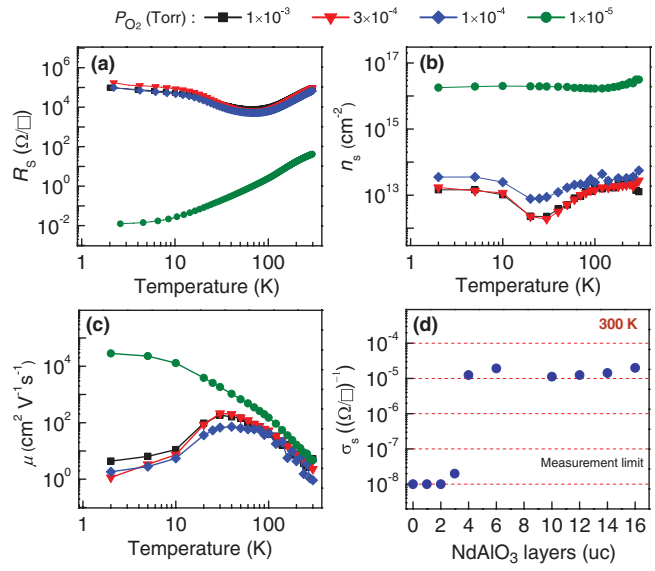

FIG. 2. (Color online) (a) Temperature dependence of the sheet resistance, $R_s(T)$, of the $NdAlO_3$/$SrTiO_3$ interfaces, for different oxygen partial pressures (P_{O_2}) during growth. Temperature dependence of (b) carrier density n_s and (c) Hall mobility μ of the $NdAlO_3$/$SrTiO_3$ interfaces. (d) Dependence of the sheet conductivity on the number of $NdAlO_3$ unit cells for the $NdAlO_3$/$SrTiO_3$ interfaces.

the P_{O_2} range of 1×10^{-3}–1×10^{-5} Torr. While all samples clearly exhibit a conducting property at their interface, the high P_{O_2} grown samples show strong upturns in R_s at lower temperatures. Interestingly, even the sample grown at P_{O_2} of 1×10^{-4} Torr shows an upturn. It is noted here that in the case of $LaAlO_3$/$SrTiO_3$ (100) interfaces such an upturn emerges only for higher P_{O_2} ($\geqslant 10^{-3}$ Torr) and "thicker" samples ($\geqslant$15 uc).[4,15] However, the sample grown at P_{O_2} of 1×10^{-5} Torr showed higher conductivity which can be understood in terms of the presence of oxygen vacancies at the interface. Figures 2(b) and 2(c) show the temperature dependence of the carrier density, n_s, and the mobility, μ, for the $NdAlO_3$/$SrTiO_3$ samples, respectively. For high P_{O_2} samples, n_s (300 K) is of the order of 4–5 $\times 10^{13}$ cm^{-2}. Whereas for sample grown at 1×10^{-5} Torr, n_s (300 K) is of the order of 10^{16} cm^{-2}, further confirming the presence of oxygen vacancies, which is a common observation for the interfaces grown at lower P_{O_2} (Refs. 16 and 17). A large carrier freeze-out towards low temperatures is observed in high P_{O_2} samples. This kind of behavior was previously observed in the cases of $LaAlO_3$/$SrTiO_3$ (Refs. 18 and 19). For all the samples, μ (300 K) is of the order of 1–8 cm^2 V^{-1} s^{-1} comparable to values reported for the $LaAlO_3$/$SrTiO_3$ (100) interfaces.[15,19] The μ follows T^2-like dependence in the temperature range of 300–100 K, behavior typical of Fermi liquid. However, a significant difference in μ is observed at low temperatures between samples grown at high and low P_{O_2}. While an abrupt drop in μ towards low temperatures is observed (which generally occurs when strong localization/magnetic scattering effects present in the system) for high P_{O_2} samples, an increase in μ throughout the temperature range down to 2 K is observed for the sample grown at 1×10^{-5} Torr.

One of the characteristic features of the 2DEG in the $LaAlO_3$/$SrTiO_3$ system is the thickness dependence of the insulator-metal transition with a critical thickness of ~4 uc of $LaAlO_3$ (Ref. 2). The sheet conductivity for the $NdAlO_3$/$SrTiO_3$ interfaces as a function of the number of unit cells of $NdAlO_3$ is depicted in Fig. 2(d), showing a clear transition from insulating to metallic interface at a thickness around 4 uc, with a change in the conductivity of more than 3 orders of magnitude across the insulator-metal transition. The similarity in the insulator-metal transition to the $LaAlO_3$/$SrTiO_3$ system confirms the formation of 2DEG at the $NdAlO_3$/$SrTiO_3$ interface and suggests that same origin for the conductivity in these interfaces. The thickness dependency of the polar layer shown here favors the idea that the electronic reconstruction could be the driving mechanism in this interface, although we cannot exclude other possible mechanisms[20,21] from our results. However, substantial differences observed in temperature dependence of n_s and μ indicate the effect of the different polar layers.

To further elucidate the polar layer effects a comparison study was carried out and samples with 10 uc $LaAlO_3$, $PrAlO_3$, and $NdGaO_3$ as the polar overlayers were grown at $P_{O_2} = 1 \times 10^{-3}$ Torr. Figure 3(a) shows the R_s variation with temperature for these various polar/nonpolar combinations. Similar to the case of $NdAlO_3$/$SrTiO_3$, $PrAlO_3$/$SrTiO_3$ interfaces also show an upturn in R_s at low temperatures. On the other hand, interestingly, $LaAlO_3$/$SrTiO_3$ and $NdGaO_3$/$SrTiO_3$ interfaces

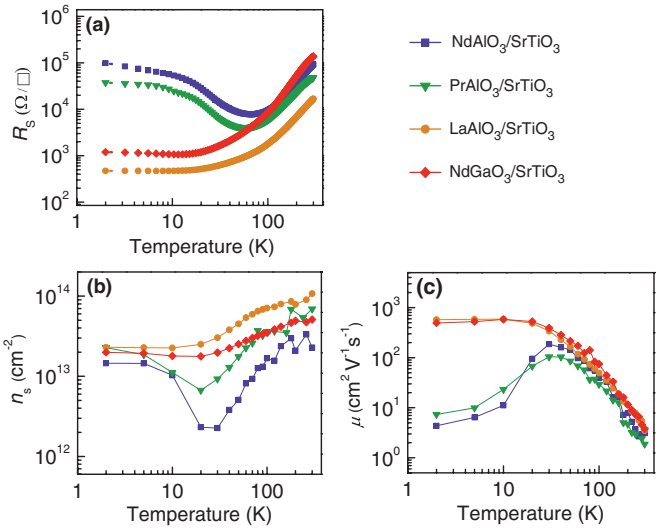

FIG. 3. (Color online) Comparison of transport properties of different polar/nonpolar ($REBO_3$/$SrTiO_3$: RE = La, Pr, or Nd; B = Al or Ga) oxide interfaces. (a) Temperature dependence of R_s of the interfaces. Temperature dependence of (b) n_s and (c) μ of the corresponding interfaces.

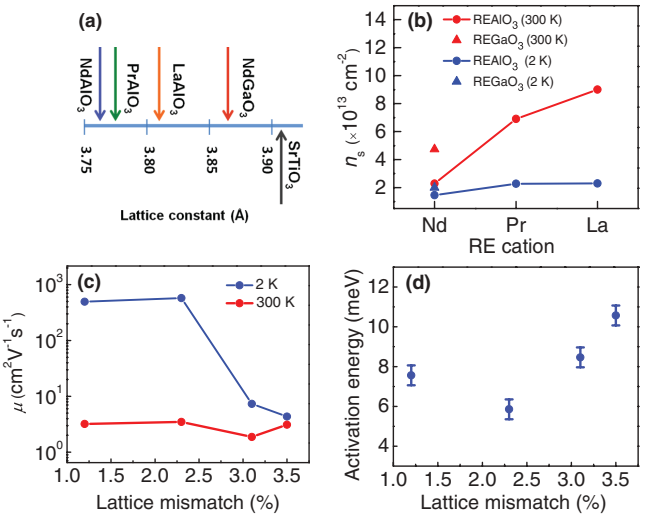

FIG. 4. (Color online) (a) Schematic diagram representing lattice parameters of different polar oxides and $SrTiO_3$. (b) n_s dependency on the RE cation of polar layers at 300 K and 2 K. (c) μ of different interfaces under lattice mismatch at 300 K and 2 K. (d) Variation in activation energy as a function of lattice mismatch.

show a typical metallic behavior without appreciable upturns in R_s. Further, their R_s at 300 K appears to have a strong dependence on the RE cation of the polar layer, where R_s is larger (∼90 kΩ) for $NdAlO_3$ compared to that of $LaAlO_3$ (∼20 kΩ). Figure 3(b) shows the n_s variation with temperature; $LaAlO_3$/$SrTiO_3$ and $NdGaO_3$/$SrTiO_3$ interfaces show minute carrier freeze-out towards low temperatures compared to $NdAlO_3$/$SrTiO_3$ and $PrAlO_3$/$SrTiO_3$ interfaces, indicating that the interfaces with $LaAlO_3$ and $NdGaO_3$ have less contribution from activated carriers. However, a carrier recovery below 15 K is observed for the $NdAlO_3$/$SrTiO_3$ and $PrAlO_3$/$SrTiO_3$ interfaces, which is possibly due to the different transport mechanism in this low temperature localized regime (further investigation is needed to understand this unusual behavior). The most remarkable effects are seen in the temperature dependence of the mobility, which is shown in Fig. 3(c). For $NdAlO_3$/$SrTiO_3$ and $PrAlO_3$/$SrTiO_3$ interfaces, μ increases initially with decreasing temperature and drops dramatically for temperatures below 40 K. On the other hand interfaces with $LaAlO_3$ and $NdGaO_3$ show an increase in μ and tend to saturate at low temperatures. An interesting observation is that even though the n_s (2 K) is nearly the same (∼2 × 10^{13} cm^{-2}) for all the interfaces, R_s and μ exhibit significant divergence, implying that the polar layer has a significant influence on the charge carriers at the polar/nonpolar interface.

Despite all of these polar layers are similar in nature, there are a few differences. First, they comprise of different chemical elements at the A site (RE cation) and the B site in the perovskite (ABO_3) structure. When the polar layer ($REBO_3$) is deposited on top of the TiO_2-terminated $SrTiO_3$ (100), the first unit cell at the interface on either side can be viewed as a stack of $REO/TiO_2/SrO$ layers. In this picture, across the interface the TiO_2 layer will have a different electronic environment in the presence of different RE cations of the polar layer. Second, different polar layers cause different lattice mismatches with $SrTiO_3$ which in turn create a different interfacial strain. To further understand these effects, we plotted the A-site cationic dependence of n_s for corresponding interfaces as shown in Fig. 4(b). Clearly n_s (300 K) is high in the case of La-based interfaces and lower for Nd-based interfaces, similar to the case of $SrTiO_3/REO/SrTiO_3$ heterostructures reported by Jang *et al.*[22] It is further shown that the electronic ground state (i.e., metallic/insulating) can be controlled by the RE cation at the interface and is attributed to the electronic correlations of the RE cation to the top $SrTiO_3$ layer, which is further supported by theoretical calculations.[22] However, n_s at 2 K has a rather small dependency on the RE cation with n_s of the order of 1–2 × 10^{13} cm^{-2} for all interfaces. The RE cation dependency of n_s shown here further suggests that the electronic effects arising from the polar layer would control the charge distribution at the interface.

Now we comment on mobility. Referring back to Fig. 3(c), the μ drop was only observed in the case of $NdAlO_3$/$SrTiO_3$ and not in the $NdGaO_3$/$SrTiO_3$ case (Nd is the A-site cation for both cases), implying that we cannot attribute this μ drop to the proximity effects of RE ions at the interface. So the only other difference these polar layers offer is the lattice mismatch at the interface with the $SrTiO_3$ substrate. Lattice mismatch here is estimated by considering in-plane lattice parameters [a schematic diagram is shown in Fig. 4(a)], among them the $NdGaO_3$/$SrTiO_3$ interface offers the least lattice mismatch (∼1.6%) and $NdAlO_3$/$SrTiO_3$ the largest (∼3.6%). Figure 4(c) shows the μ variation with lattice mismatch; here μ (300 K) shows modest dependency on the lattice mismatch with values typically of the order of 1–5 cm^2 V^{-1} s^{-1}, which suggests the predominant electron-phonon scattering at 300 K. In contrast, μ (2 K) shows strong dependence on the lattice mismatch: μ is ∼500 cm^2 V^{-1} s^{-1} for $NdGaO_3$/$SrTiO_3$ and only 4 cm^2 V^{-1} s^{-1} for $NdAlO_3$/$SrTiO_3$ (a drop of a factor of 100). It appears that the large lattice mismatch is limiting the μ.

Recent reports on $LaAlO_3/SrTiO_3$ interface using high-resolution transmission electron microscopy[23] and x-ray diffraction[24] show that in the top layers of $SrTiO_3$ the Ti octahedra are distorted, which strongly implies that the top few layers of $SrTiO_3$ are under the influence of strain provided by the polar overlayers through structural coupling across the interface. The fundamental issue here is that the charge carriers occupy the Ti site and predominantly reside in the top few layers of $SrTiO_3$ and various polar layers offer a range of degrees of distortion in the top layers of $SrTiO_3$ due to the lattice mismatch. Therefore the degree of strain/distortion in these $SrTiO_3$ layers can be expected to play a crucial role in manipulating electronic properties at the interface. Therefore the mobility variation observed here can be ascribed to the degree of strain induced in $SrTiO_3$ layers by lattice mismatch. Further we note here that, even though the carrier density (n_s) at 2 K is almost the same ($\sim 2 \times 10^{13}$ cm^{-2}) for all interfaces, a large variation in μ is observed, suggesting that e-e interactions play a key role in these various interfaces. Thus, we propose that the combined effects of strain and electron correlations are crucial in controlling μ. Further, because of a smaller lattice mismatch a higher μ is expected in the case of $NdGaO_3$ ($\sim$1.6%) compared to the case of $LaAlO_3$ (mismatch $\sim$2.3%) due to lesser mismatch; however, the mobility values are just comparable in both cases. We attribute this to the residual impurity scattering in $SrTiO_3$ itself.

As mentioned earlier a large carrier freeze-out is observed for the carriers with temperature. To examine this, we extracted activation energy from Arrhenius plots (between 20 K and 300 K) of the n_s versus temperature graphs in Fig. 3(b). Activation energies of the order of a few meV are in agreement with the previous report on $LaAlO_3/SrTiO_3$[19]. Figure 4(d) shows activation energy as a function of lattice mismatch. Interestingly, activation energy gradually increases with lattice mismatch and it is largest (16 meV) for the $NdAlO_3/SrTiO_3$ interface. In general, the activation energy indicates the relative position of the carrier donor level from the conduction band in the energy scale. Its variation with lattice mismatch may suggest a relative shift in the position of the donor level among these interfaces. Recently, it has been proposed that strain could leads to distortion of Ti octahedra through octahedral rotation/tilt in $SrTiO_3$-based heterostructures,[23,24] which in turn could alter the position of energy levels. Since electronic effects are quite sensitive to the degree of octahedral distortion, it is further interesting to study the effects of octahedral distortions on novel phases at these interfaces.

IV. CONCLUSION

In conclusion, we demonstrate the observation of 2DEG at the $NdAlO_3/SrTiO_3$, $PrAlO_3/SrTiO_3$, and $NdGaO_3/SrTiO_3$ interfaces and, further, the observed thickness dependence of the metal-insulator transition suggests that polar discontinuity may possibly be the prime origin of conductivity at these polar/nonpolar interfaces. The combined effects of interface strain and electron correlations offered by polar layers seem to control the carrier density and mobility of 2DEG. Moreover the presence of large octahedral distortions due to interface strain may play an important role in manipulating the novel phases at the interface. Our observations further emphasize the key role of polar layers in these heterostructures and may provide an opportunity to tune the properties at selected polar/nonpolar oxide interfaces.

ACKNOWLEDGMENTS

We thank the National Research Foundation (NRF), Singapore, under the Competitive Research Program (CRP) "Tailoring Oxide Electronics by Atomic Control" (Grant No. NRF2008NRF-CRP002-024), the National University of Singapore (NUS) for a cross-faculty grant, and the FRC (ARF Grant No. R-144-000-278-112) for financial support.

*ariando@nus.edu.sg

[1] A. Ohtomo and H. Y. Hwang, Nature (London) **427**, 423 (2004).
[2] S. Thiel, G. Hammerl, A. Schmehl, C. W. Schneider, and J. Mannhart, Science **313**, 1942 (2006).
[3] N. Reyren, S. Theil, A. D. Caviglia, L. Fitting Kourkoutis, G. Hammer, C. Richter, C. W. Schneider, T. Kopp, A.-S. Ruetschi, D. Jaccard, M. Gabay, D. A. Muller, J.-M. Triscone, and J. Mannhart, Science **317**, 1196 (2007).
[4] A. Brinkman, M. Huijben, M. Van Zalk, J. Huijben, U. Zeitler, J. C. Maan, W. G. Van der Wiel, G. Rijinders, D. H. A. Blank, and H. Hilgenkamp, Nat. Mater. **6**, 493 (2007).
[5] Ariando, X. Wang, G. Baskaran, Z. Q. Liu, J. Huijben, J. B. Yi, A. Annadi, A. Roy Barman, A. Rusydi, S. Dhar, Y. P. Feng, J. Ding, H. Hilgenkamp, and T. Venkatesan, Nat. Commun. **2**, 188 (2011).
[6] C. Cen, S. Thiel, G. Hammerl, C. W. Schneider, K. E. Andersen, C. S. Hellberg, J. Mannhart, and J. Levy, Nat. Mater. **7**, 298 (2008).
[7] Y. Xie, Y. Hikita, C. Bell, and H. Y. Hwang, Nat. Commun. **2**, 494 (2011).
[8] C. W. Bark. D. A. Felker, Y. Wang, Y. Zhang, H. W. Jang, C. M. Folkman, J. W. Park, S. H. Baek, H. Zhou, D. D. Fong, X. Q. Pan, E. Y. Tsymbal, M. S. Rzchowski, and C. B. Eom, Proc. Natl. Acad. Sci. USA **108**, 4720 (2011).
[9] C. Cancellieri, D. Fontaine, S. Gariglio, N. Reyren, A. D. Caviglia, A. Fete, S. J. Leake, S. A. Pauli, P. R. Willmott, M. Stengel, Ph. Ghosez, and J.-M. Triscone, Phys. Rev. Lett. **107**, 056102 (2011).
[10] C. W. Bark, P. Sharma, Y. Wang, S. H. Baek, S. Lee, S. Ryu, C. M. Folkman, T. R. Paudel, A. Kumar, S. V. Kalinin, A. Sokolov, E. Y. Tsymbal, M. S. Rzchowski, A. Gruverman, and C. B. Eom, Nano Lett. (2012), doi:10.1021/nl3001088.
[11] P. Perna, D. Maccariello, M. Radovic, U. Scotti di Uccio, I. Pallecchi, M. Codda, D. Marr, C. Cantoni, J. Gazquez, M. Varela, S. J. Pennycook, and F. Miletto Granozio, Appl. Phys. Lett. **97**, 152111 (2010).
[12] N. Nakagawa, H. Y. Hwang, and D. A. Muller, Nat. Mater. **5**, 204 (2006).
[13] M. Kawasaki, K. S. Takahashi, T. Maeda, R. Tsuchiya, M. Shinohara, O. Ishiyama, T. Yonezawa, M. Yoshimoto, and H. Koinuma, Science **266**, 1540 (1994).

[14]G. Koster, B. L. Kropman, G. J. H. M. Rijinders, D. H. A. Blank, and H. Rogalla, Appl. Phys. Lett. **73**, 2920 (1998).
[15]C. Bell, S. Harashima, Y. Hikita, and H. Y. Hwang, Appl. Phys. Lett. **94**, 222111 (2009).
[16]W. Siemons, G. Koster, H. Yamamoto, T. H. Geballe, D. H. A. Blank, and M. R. Beasley, Phys. Rev. B **76**, 155111 (2007).
[17]A. Kalabukhov, R. Gunnarsson, J. Borjesson, E. Olsson, T. Claeson, and D. Winkler, Phys. Rev. B **75**, 121404 (R) (2007).
[18]M. Huijben, G. Koster, H. J. A. Molegraaf, M. K. Kruize, S. Wenderich, J. E. Kleibeuker, A. McCollam, V. K. Guduru, A. Brinkman, H. Hilgenkamp, U. Zeitler, J. C. Maan, D. H. A. Blank, and G. Rijnders, arXiv:1008.1896.
[19]M. Huijben, G. Rijinders, D. H. A. Blank, S. Bals, S. V. Aert, J. Verbeeck, G. V. Tendeloo, A. Brinkman, and H. Hilgenkamp, Nat. Mater. **5**, 556 (2006).
[20]W. Siemons, G. Koster, H. Yamamoto, W. A. Harrison, G. Lucovsky, T. H. Geballe, D. H. A. Blank, and M. R. Beasley, Phys. Rev. Lett. **98**, 196802 (2007).
[21]P. R. Willmott, S. A. Pauli, R. Herger, C. M. Schleputz, D. Matroccia, B. D. Patterson, B. Delley, R. Clarke, D. Kumah, C. Cionca, and Y. Yacoby, Phys. Rev. Lett. **99**, 155502 (2007).
[22]H. W. Jang, D. A. Felker, C. W. Bark, Y. Wang, M. K. Niranjan, C. T. Nelson, Y. Zhang, D. Su, C. M. Folkman, S. H. Baek, S. Lee, K. Janicka, Y. Zhu, X. Q. Pan, D. D. Fong, E. Y. Tsymbal, M. S. Rzchowski, and C. B. Eom, Science **331**, 886 (2011).
[23]C. L. Jia, S. B. Mi, M. Faley, U. Poppe, J. Schubert, and K. Urban, Phys. Rev. B **79**, 081405(R) (2009).
[24]J. E. Boschker, C. Folkman, C. W. Bark, A. F. Monsen, E. Folven, J. K. Grepstad, E. Wahlstrom, C. B. Eom, and T. Tybell, Phys. Rev. B **84**, 205418 (2011).